Determination of double-*G* energy fracture criterion for concrete materials

Zhao Yanhua & Xu Shilang
Department of Civil Engineering, Dalian University of Technology, China

ABSTRACT: In parallel to double-*K* fracture model, double-*G* energy criterion based on the energy release rate is proposed, where two pivotal fracture parameters are introduced: the initial fracture toughness $G_{\mathrm{Ic}}^{\mathrm{ini}}$ and the unstable fracture toughness $G_{\mathrm{Ic}}^{\mathrm{un}}$, which enable us to distinguish three stages manifested during crack propagation procedure. Moreover, these two parameters are not independent, the discrepancy between them is $G_{\mathrm{Ic}}^{\mathrm{c}}$, the energy assumption devoted by cohesive force distributed throughout the fracture process zone (FPZ). Investigation into the double-*G* energy parameters together with double-*K* fracture parameters provides that when an equivalent elastic traction-free crack plus an equivalent elastic fictitious crack zone is considered, these fracture parameters still follow the same conversion principle as stated in linear elastic fracture mechanics (LEFM). Accordingly, the double-*G* energy fracture criterion can be deemed as a supplement to the double-*K* fracture model in describing the crack propagation in concrete materials.

Keywords: concrete, double-*K* fracture model, fracture process zone, fracture toughness, cohesive force

1 INTRODCUTION

Fictitious crack model (Hillerborg, 1976) signified the incipience of nonlinear fracture mechanics study for concrete. In this model, normal stresses, also known as cohesive forces, are transmitted along the FPZ ahead of the traction-free crack. Now it is well-received that the very existence of FPZ is responsible for the unsuccessful application of linear elastic fracture mechanics for concrete-like quasibrittle materials. In mid 1980s, another fracture model of significance was proposed by Bažant, nay, crack band model (Bažant, 1983) which is now extensively used in practice for fracture analysis of concrete material because of its convenient programming and consideration of triaxial stresses. To predict the crack extension and the influence of FPZ upon the fracture characteristics, still many other facture models applicable to quasibrittle materials have been suggested, to name but a few, the two parameter fracture model (Jenq et al. 1985), the effective crack model (Karihaloo et al. 1990, Swartz et al, 1987), size effect model (Bažant, 1986). Among most of these models, fracture toughness K_{Ic}(here subscript I indicates the Mode-I fracture pattern) is presented to predict the critical unstable state. The single parameter K_{Ic}, measuring the magnitude of crack extension resistance, is sufficient for normal concrete structures design and service requirement. While in some special cases, such as a concrete pressure vessel or a huge concrete dam, crack initiation is somehow posing the same significance as the unstable crack propagation, and what's more in some cases, the prediction of crack initiation is still much more important. In view of this, Xu and Reinhardt developed double-*K* criterion(Xu et al. 1999) where two fracture toughnesses ($K_{\mathrm{Ic}}^{\mathrm{ini}}$ and $K_{\mathrm{Ic}}^{\mathrm{un}}$)are introduced. $K_{\mathrm{Ic}}^{\mathrm{ini}}$, termed as the initial fracture toughness, implies the inherent crack extension resistance of material in the absence of FPZ; while $K_{\mathrm{Ic}}^{\mathrm{un}}$ is set to the unstable fracture toughness marking the critical state when the crack begins unstable failure. With these two vital parameters, three different stages that a crack may experience can be clearly distinguished: crack initiation, stable crack propagation and unstable failure. Apart from conceptual manifestation, the testing procedure to determine double-K fracture parameters is very simple without unloading and reloading cycle, only a monotonous loading is needed until the maximum load is attained, and thus a closed-loop testing system is not necessary. For most common materials and structural laboratories, this method is rather easy to perform.

Two different modeling techniques are often used in the field of fracture mechanics to describe when materials fail: the stress intensity approach and the energy approach. In the former case, the stress intensity factor K at one crack/flaw tip is taken as a measurement of material state: when it exceeds the intrinsic fracture toughness K_{Ic} of material, the material fails. Accordingly, many of the models suitable for concrete mentioned above will fall into this category. While for the energy method hinged on the energy release rate G (or crack driving force), the governing fracture parameter is stated as a critical energy release rate G_{Ic}. For a homogeneous brittle material where LEFM can be successfully applied, these two methods are equivalent: K and G are not independent parameters, that is to say, between them certain relationship must exist which is available from LEFM. And K_{Ic} and G_{Ic} are both indistinctively called fracture toughness. While for concrete-like quasibrittle materials which LEFM are not suitable to directly apply, one question may arise with respect to the relation between two fracture toughness, viz. K_{Ic} and G_{Ic}, whether they are still equivalent in determining the fracture properties of concrete, if so, they whether or not follow the same principal as in LEFM.

Inspired by the double-K fracture model, the primary objective of this article is to establish the fracture toughness from the viewpoint of energy consideration in terms of the energy release rate G. In parallel to double-K fracture parameters, two energy-oriented counterparts $G_{\mathrm{Ic}}^{\mathrm{ini}}$ and $G_{\mathrm{Ic}}^{\mathrm{un}}$ (the initial fracture toughness and unstable fracture toughness respectively) are presented here. And energy consumption $G_{\mathrm{Ic}}^{\mathrm{c}}$ over the FPZ correlates these two fracture toughness parameters, which at the same time provides a practical approach for determining them.

2 LINEAR ASYMPTOTIC SUPERPOSITION ASSUMPTION

It is now generally accepted that the non-linearity observed in the ascending branch of load-deflection response of materials can be attributed to the neglecting of FPZ existence ahead of the traction-free crack tip. Since LEFM is well established and easy to apply, most researchers made their efforts to find out conjunction between LEFM and the nonlinear fracture behavior of concrete-like quasibrittle materials. Then LEFM can be satisfactorily extended to this kind of material. With this in mind, most of those fracture models suitable for quasibrittle materials treated the FPZ in the vicinity of the crack tip as an equivalent linear-elastic fictitious crack based on various postulations. And this method can be regarded as a modified LEFM approach. Double-K fracture model, in the sense, is such an improved LEFM method in conjunction with fictitious crack model as clearly seen in the two following hypotheses introduced in linear asymptotic superposition assumption (Xu et al. 1998):

1. the nonlinear characteristics on *P-CMOD* curve is caused by the fictitious crack extension in front of a stress-free crack;
2. an effective crack consists of an equivalent-elastic stress-free crack and an equivalent elastic fictitious crack extension.

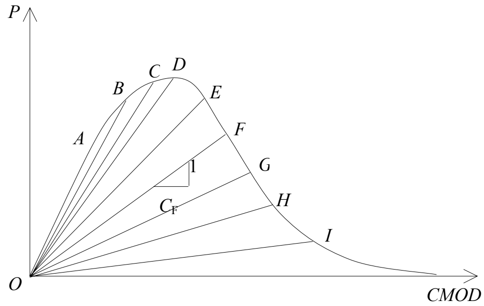

Fig. 1 The sketch of linear asymptotic superposition of *P-CMOD* curve

According to the linear asymptotic superposition assumption, the whole fracture procedure considering the non-linearity can be described from LEFM point of view: a typical load-displacement curve can be taken as an assembly of a series of linear elastic points, consequently LEFM can be utilized to identify fracture behavior of concrete.

3 DOUBLE-*G* ENERGY CRITERION ESTABLISHMENT

It was just the energy method that Griffith adopted in his first successful analysis of a fracture mechanics problem. He made the point that there was a simple energy balance consisting of a decrease in elastic strain energy within the stressed body as the crack extends counteracted by the energy needed to create new crack surface. And because of complexity, it developed somewhat slowly comparing to the stress intensity method, as testified by many of fracture models which adopted the stress intensity factor *K* as their fracture determinant parameter. So was the case with Double-*K* fracture model. When energy description is needed for some cases, however, these models cannot be directly applied. Inspired by the Double-*K* fracture model, energy-oriented fracture model in terms of energy release rate *G* is listed as

$$\begin{aligned} &G < G_{\mathrm{Ic}}^{\mathrm{ini}}, && \text{crack remains unchanged} \\ &G = G_{\mathrm{Ic}}^{\mathrm{ini}}, && \text{crack initiation} \\ &G_{\mathrm{Ic}}^{\mathrm{ini}} < G < G_{\mathrm{Ic}}^{\mathrm{un}}, && \text{crack stable propagation} \\ &G = G_{\mathrm{Ic}}^{\mathrm{un}}, && \text{crack critical unstable state} \\ &G > G_{\mathrm{Ic}}^{\mathrm{un}}, && \text{crack failure} \end{aligned} \qquad (1)$$

Here two energy-oriented fracture parameters $G_{\mathrm{Ic}}^{\mathrm{ini}}$ and $G_{\mathrm{Ic}}^{\mathrm{un}}$ act as the controlling quantities of the entire fracture procedure. $G_{\mathrm{Ic}}^{\mathrm{ini}}$, termed as the initial fracture toughness, implies the inherent toughness of material corresponding to the initiation load P_{ini} and the initiation crack length a_0. The material behavior is linear elastic prior to the attainment of $G_{\mathrm{Ic}}^{\mathrm{ini}}$. In this stage, the load-bearing body stores the reversible strain energy when the load increases, but the crack length remains unchanged at a_0. The instant the energy release rate *G* achieves $G_{\mathrm{Ic}}^{\mathrm{ini}}$, the crack growth commences, signifying the incipience of non-linearity observed in the load-displacement curve. For some structures calling for strict crack growth control, especially for concrete structures to protect the environment against pollution necessitating the exact evaluation of crack initiation, $G_{\mathrm{Ic}}^{\mathrm{ini}}$ can be figured as the criterion for crack propagation. When the crack spreads forward in a stable way, the energy release rate *G* at any time is greater than $G_{\mathrm{Ic}}^{\mathrm{ini}}$ and less than $G_{\mathrm{Ic}}^{\mathrm{un}}$, where $G_{\mathrm{Ic}}^{\mathrm{un}}$ is defined as the unstable fracture toughness. FPZ during this stage is assumed to propagate stably with increasing load until the maximum load $P_{\max}$ and the critical crack mouth opening displacement $CMOD_{\mathrm{c}}$ simultaneously reached for type-G test[3] which is just so for many testing specimens. Generally, $G_{\mathrm{Ic}}^{\mathrm{un}}$ is treated as fracture criterion for a normal structure. After this critical unstable state, the crack tip propagates in an unstable manner until the termination at the end point of *P-CMOD* curve. In practical engineering application, different safety criterion can be selectively adopted according to various structure safety requests analogous to that in double-*K* fracture model (Xu, 2002).

4 DOUBLE-G FRACTURE PARAMETERS COMPUTATION

With the aid of the linear asymptotic superposition assumption, LEFM can be exploited to compute double-*G* fracture parameters. So $G_{\mathrm{Ic}}^{\mathrm{ini}}$ and $G_{\mathrm{Ic}}^{\mathrm{un}}$ can be evaluated using formula developed in LEFM

$$G = \frac{P^2 dC}{2Bda} \qquad (2)$$

where *B* is the thickness of specimen; $C=\delta/P$ is the compliance in the load-displacement curve. The Eq.(2) shows that the extension in the crack length will bring the change in the compliance, then forward to the change in the energy release rate with the body. Eq.(2) gives the explicit relation between *G* and the compliance *C*. This equation is an important basis for determining the *G* values. Once the load-displacement P-δ diagram is recorded, numerical value *dC/da* may be obtained, then the energy release rate *G* at any time can be obtained analytically from Eq.(2).

From the previous analysis, the double-*G* fracture parameters $G_{\mathrm{Ic}}^{\mathrm{ini}}$ and $G_{\mathrm{Ic}}^{\mathrm{un}}$ can be directly evaluated by inserting the relevant quantities into Eq.(2) respectively. In details: $G_{\mathrm{Ic}}^{\mathrm{ini}}$ can be evaluated by substituting initial crack load P_{ini} and the pre-existing crack length a_0 into Eq.(2); similarly, the unstable fracture toughness $G_{\mathrm{Ic}}^{\mathrm{un}}$ can be calculated by introducing the maximum $P_{\max}$ and the critical crack length a_{c}.

Particularly noteworthy, in practical testing procedure for determining those two fracture toughness, the results of maximum load $P_{\max}$ has much lower scatter and can be easily and unambiguously interpreted. Comparing to that, however, the accurate choice of initial crack load P_{ini} may be a tough task. Conceptually, the P_{ini} value is at the end of the linear segment of the measured P-δ curve, but this point is very difficult to locate. In view of this, an alternative expression for $G_{\mathrm{Ic}}^{\mathrm{ini}}$ is provided by lead-in concept of energy consumption $G_{\mathrm{Ic}}^{\mathrm{c}}$ over the FPZ.

From the foregoing linear asymptotic superposition assumption, the critical effective crack length a_c is composed of two parts: the pre-existing crack length a_0 and the effective crack extension Δa_c. Cohesive forces, representing the forces transmitted across the FPZ, are distributed conforming to the traction-separation constitutive relation associated with the crack opening displacement. During the stable crack propagation process, the energy consumption includes two parts: the first is $G_{\mathrm{Ic}}^{\mathrm{ini}}$ for the crack initiation, the other portion is the work performed on the cohesive forces denoted as $G_{\mathrm{Ic}}^{\mathrm{c}}$. Mathematically speaking, this relation can be written as

$$G_{\mathrm{Ic}}^{\mathrm{un}} = G_{\mathrm{Ic}}^{\mathrm{ini}} + G_{\mathrm{Ic}}^{\mathrm{c}} \tag{3}$$

Note the $G_{\mathrm{Ic}}^{\mathrm{c}}$ only correlates with the distribution of cohesive force along the FPZ. Eq.(3) offers an alternative to ascertain the value of $G_{\mathrm{Ic}}^{\mathrm{ini}}$.

5 THE ENERGY CONSUMPTION $G_{\mathrm{Ic}}^{\mathrm{c}}$ OVER FPZ

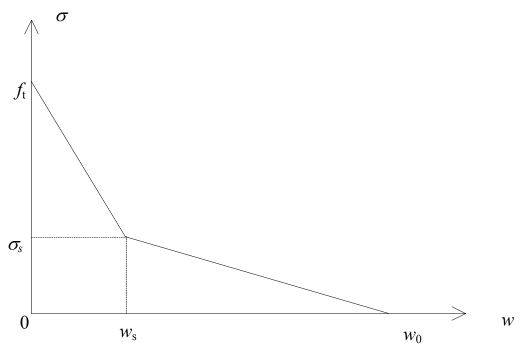

Fig.2 A bilinear softening traction-separation curve

The softening traction-separation law is prerequisite in determining the distribution of cohesive force along the FPZ. For the simplicity of numerical computation, a bilinear form is generally adopted to determine this softening traction-separation relation. By making reference to Fig.2, the appropriate expression for constitutive relation within the fracture process zone can be written

$$\begin{aligned} &\sigma = f_t - (f_t - \sigma_s)\frac{w}{w_s} && 0 \leqslant w \leqslant w_s \\ &\sigma = \sigma_s \frac{w_0 - w}{w_0 - w_s} && w_s \leqslant w \leqslant w_0 \\ &\sigma = 0 && w_0 \leqslant w \end{aligned} \tag{4}$$

For numerical and analytical analysis, three parameters, the transition coordinate(σ_s, w_s) and the terminal point w_0 , should be carefully chosen. Herein, a refined determination method based on concrete grade and aggregate maximum dimension $d_{\max}$ that has good agreement with the corresponding data normalized in CEB-FIP Model Code 1990(CEB, 1993) is given as follows(Xu, 1999)

$$\begin{aligned} &\lambda = 10 - \left[f_{\mathrm{ck}} / (2 f_{\mathrm{ck0}})\right]^{0.7} \\ &\alpha_{\mathrm{F}} = \lambda - d_{\max}^{0.9}/8 \\ &G_{\mathrm{F}} = (0.0204 + 0.0053 d_{\max}^{0.95}/8)(f_c / f_{c0}) \end{aligned} \tag{5}$$

$$\begin{aligned} &w_0 = \alpha_{\mathrm{F}} G_{\mathrm{F}} / f_t \\ &w_s = 0.4\sqrt{\alpha_{\mathrm{F}}} G_{\mathrm{F}} / f_t \\ &\sigma_s = (2 - 0.4\sqrt{\alpha_{\mathrm{F}}}) f_t / \alpha_{\mathrm{F}} \end{aligned} \tag{6}$$

where f_t、f_c are tensile strength and compressive strength in MPa respectively, and f_t=0.4983$(f_c)^{1/2}$, f_{c0}=10MPa；f_{ck} , the characteristic strength to represent the concrete grade in MPa, equal to (f_c-8) MPa according to CEB-FIP Model Code 1990；f_{ck0}=10 MPa.

At the critical unstable state, the distribution of cohesive force over the FPZ exhibits different shape according to the relation between $CTOD_c$ (acronym for crack tip opening displacement) and the turning point value w_s at the softening curve. Two more general cases are as follows: When $CTOD_c \leqslant w_s$, the distribution is illustrated as Fig.3; while for $w_s \leqslant CTOD_c \leqslant w_0$, the distribution is in Fig.4.

The average energy dissipated by the cohesive force over FPZ at the critical unstable state, or the work needed to perform on the cohesive force by unit area can be expressed as

$$\begin{aligned} &G_{\mathrm{Ic}}^{\mathrm{c}} = \frac{1}{a_c - a_0}\int_{a_0}^{a_c} \Gamma(x)dx \\ &\Gamma(x) = \int_0^{w_x} \sigma(w)dw \end{aligned} \tag{7}$$

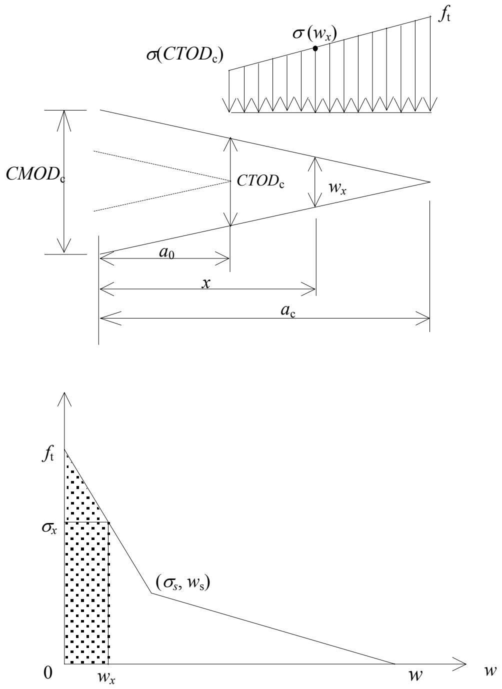

Fig.3 The distribution of cohesive force along the FPZ for $CTOD_c \leqslant w_s$

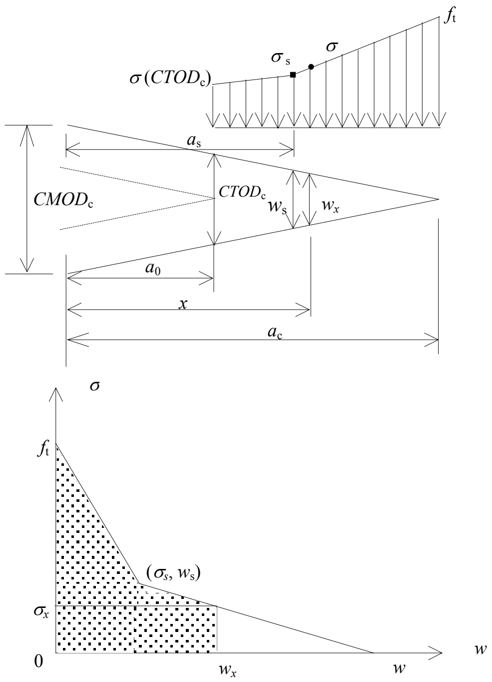

Fig.4 The distribution of cohesive force along the FPZ for $w_s \leqslant CTOD_c \leqslant w_0$

where x=coordinate measured from the crack mouth; a_0 and a_c are the pre-existing notch and critical crack length respectively; $\Gamma(x)$=local fracture energy, implying the energy exhaustion at distance x from the crack mouth when the crack opening displacement transforms from 0 to w_x. Clearly this energy is mainly dissipated within the FPZ instead of being used in creating the new smooth fracture surfaces as described in physics and thermodynamics (Bažant , 1996; Nallathambi, 1984).

Due to the different distribution of cohesive force σ over FPZ, the accurate expression for $G_{\mathrm{Ic}}^{\mathrm{c}}$ is different, which will be discussed in greater detail in the following section.

For the case of $CTOD_c \leqslant w_s$, the distribution of cohesive force σ is shown in Fig.3, and the expression for $G_{\mathrm{Ic}}^{\mathrm{c}}$ from Eq.(7) may be rewritten as

$$\begin{cases} G_{\mathrm{Ic}}^{\mathrm{c}} = \dfrac{1}{a_{\mathrm{c}} - a_0} \displaystyle\int_{a_0}^{a_{\mathrm{c}}} \Gamma(x) dx \\ \Gamma(x) = \displaystyle\int_0^{w_x} \sigma(w) dw = \dfrac{f_t + \sigma_x}{2} w_x \\ \sigma_x = f_{\mathrm{t}} - (f_{\mathrm{t}} - \sigma_{\mathrm{s}}) \dfrac{w_x}{w_{\mathrm{s}}} \end{cases} \tag{8}$$

where the local fracture energy $\Gamma(x)$ is the shaded area in Fig.3; whereas the stress σ_x at coordinate x is obtained from the softening traction-separation law in Eq.(4).

Likewise, the distribution of cohesive force σ over the FPZ can be divided into two regions (a_0, a_s) and (a_s, a_c) for the case of $w_s \leqslant CTOD_c \leqslant w_0$, wherein a_s is the distance from crack mouth where the crack opening displacement at this point is up to w_s. Then the expression for $G_{\mathrm{Ic}}^{\mathrm{c}}$ from Eq.(7) can be reformulated as

$$\begin{aligned} G_{\mathrm{Ic}}^{\mathrm{c}} &= \frac{1}{a_{\mathrm{c}} - a_0} \int_{a_0}^{a_{\mathrm{c}}} \Gamma(x) dx \\ &= \frac{1}{a_{\mathrm{c}} - a_0} \left(\int_{a_0}^{a_{\mathrm{s}}} \Gamma_1(x_1) dx_1 + \int_{a_s}^{a_{\mathrm{s}}} \Gamma_2(x_2) dx_2 \right) \end{aligned} \tag{9}$$

where $\Gamma_1(x_1)$, the local fracture energy dissipated within the span (a_0, a_s), corresponds to the shaded area in Fig.4 because of the condition $w_{x_1} \geqslant w_s$ is satisfied. This may produce

$$\begin{aligned} &\Gamma_1(x_1) = \frac{f_{\mathrm{t}} + \sigma_{\mathrm{s}}}{2} w_{\mathrm{s}} + \frac{\sigma_{\mathrm{s}} + \sigma_{x_1}}{2} (w_{x_1} - w_{\mathrm{s}}) \\ &\sigma_{x_1} = \sigma_{\mathrm{s}} \frac{w_0 - w_{x_1}}{w_0 - w_{\mathrm{s}}} \end{aligned} \tag{10}$$

$\Gamma_2(x_2)$ in the second term of right hand of Eq.(9) is energy consumption within the region (a_s, a_c).

Considering $w_{x_2} \leqslant w_s$ in this region, reference can be made to Fig.3 to get the expression for $\Gamma_2(x_2)$

$$\Gamma_2(x_2) = \frac{f_t + \sigma_{x_2}}{2} w_{x_2}$$
$$\sigma_{x_2} = f_t - (f_t - \sigma_s)\frac{w_{x_2}}{w_s} \tag{11}$$

For general situation at the critical state, $w_0 \leqslant CTOD_c$ rarely occurs, therefore this case will not be analyzed here.

6 TEST VERIFICATION OF DOUBLE-*K* FRACTURE PARAMETERS AND DOUBLE-*G* FRACTURE PARAMETERS

6.1 Determination of double-G fracture parameters from CT *(compact tension) specimen*

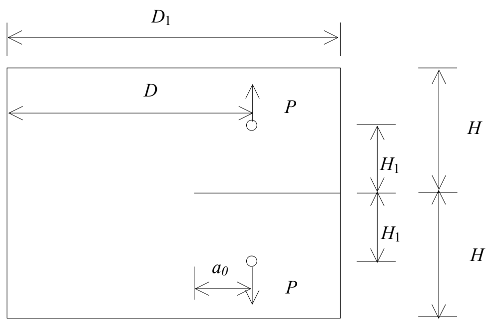

Fig.5 The configuration of the compact tension specimen

For the standard compact tension specimen (Fig.5) recommended by ASTM standard E-399-72 (ASTM, 1972), the loading line crack opening displacement *COD* can be expressed with 0.5 percent accuracy for $0.2 \leqslant a/D \leqslant 0.975$ as follows (Murakami, 1987)

$$COD = PV(\alpha)/BE$$
$$V(\alpha) = (\frac{1+\alpha}{1-\alpha})^2 (2.163 + 12.219\alpha - 20.065\alpha^2 - 0.9925\alpha^3 + 20.609\alpha^4 - 9.9314\alpha^5) \tag{12}$$

where $\alpha = a/D$; B and E are the specimen thickness and material elastic modulus respectively. After some algebraic transformatins, the variation of compliance $C=COD/P$ with respect to the increment of crack length da can be reformulated through Eq.(12)

$$\frac{dC}{d\alpha}BE = \frac{4(1+\alpha)}{(1-\alpha)^3}(2.163 + 12.219\alpha - 20.065\alpha^2 - 0.9925\alpha^3 + 20.609\alpha^4 - 9.9314\alpha^5) + (\frac{1+\alpha}{1-\alpha})^2 (12.219 - 40.13\alpha - 2.9775\alpha^2 + 82.436\alpha^3 - 49.657\alpha^4) \tag{13}$$

According to the previous analysis, the critical effective crack length $\alpha_c = a_c/D$ can be obtained from Eq.(12) with the measured value P_{max} and the corresponding crack opening displacement COD_c. Then the unstable fracture toughness G_{Ic}^{un} can be obtained easily by substituting P_{max} and the critical effective value α_c solved above into Eq.(13)and Eq.(2).

For computational convenience of energy dissipation G_{Ic}^{c} over the FPZ, let $y=x/a_c$, then Eq.(8) for the case of $CTOD_c \leqslant w_s$ can be expressed in a dimensionless way

$$\begin{cases} G_{Ic}^{c} = \dfrac{a_c \times f_t \times CMOD_c}{a_c - a_0}\displaystyle\int_{a_0/a_c}^{1} \frac{1+\sigma_y/f_t}{2}\frac{w_y}{CMOD_c}dy \\ \dfrac{w_y}{CMOD_c} = \sqrt{(1-y)^2 + (1.081 - 1.149y)(y - y^2)} \\ \dfrac{\sigma_y}{f_t} = 1 - (1 - \dfrac{\sigma_s}{f_t})\dfrac{w_y}{w_s} = 1 - (1 - \dfrac{\sigma_s}{f_t})\dfrac{w_y/CMOD_c}{w_s/CMOD_c} \end{cases} \tag{14}$$

Similarly, the Eq.(9) for case $w_s \leqslant CTOD_c \leqslant w_0$ can be rewritten in the following form

$$\begin{cases} G_{Ic}^{c} = \dfrac{a_c \times f_t \times CMOD_c}{a_c - a_0}\left\{\displaystyle\int_{a_s/a_c}^{1} \frac{1+\sigma_{y_2}/f_t}{2}\frac{w_{y_2}}{CMOD_c}dy_2 + \int_{a_0/a_c}^{a_s/a_c} \frac{1+\sigma_s/f_t}{2}\frac{w_s}{CMOD_c} + \frac{\sigma_s/f_t + \sigma_{y_1}/f_t}{2}(\frac{w_{y_1}}{CMOD_c} - \frac{w_s}{CMOD_c})dy \right\} \\ \dfrac{\sigma_{y_1}}{f_t} = \dfrac{\sigma_s}{f_t}\dfrac{w_0/CMOD_c - w_{y_1}/CMOD_c}{w_0/CMOD_c - w_s/CMOD_c} \\ \dfrac{\sigma_{y_2}}{f_t} = 1 - (1 - \dfrac{\sigma_s}{f_t})\dfrac{w_{y_2}/CMOD_c}{w_s/CMOD_c} \\ \dfrac{w_{y_1}}{CMOD_c} = \sqrt{(1-y_1)^2 + (1.081 - 1.149y_1)(y_1 - y_1^2)} \\ \dfrac{w_{y_2}}{CMOD_c} = \sqrt{(1-y_2)^2 + (1.081 - 1.149y_2)(y_2 - y_2^2)} \end{cases} \tag{15}$$

So far the unstable fracture toughness G_{Ic}^{un} , the fracture energy G_{Ic}^{c} over FPZ and the initial fracture toughness G_{Ic}^{ini} can be computed with the aid of Eq.(3).

Using the testing results (Xu, 1999) of CT specimen involving the maximum load P_{max} and its corresponding crack opening displacement COD_c in Table 1, the two main fracture parameters: the unstable fracture toughness G_{Ic}^{un} and the initial fracture toughness G_{Ic}^{ini} can be quantified by the method mentioned above.

Table 1 The experimental results from compact tension specimen (a_0/D=0.5)

	Mechanical parameters	Specimen dimension $D\times 2H\times B$(m)	P_{max} (KN)	COD_c (μm)
1	f_c=42.9MPa E=31.0Gpa f_t=3.264MPa	1.2×1.4×0.12	22.15	356.1
2			21.25	309.1
3			21.	378.2
4			20.55	372.7
5			20.32	310.9
6			19.	291.5
7		0.6×0.72×0.12	13.	216.7
8			12.9	227.3
9			12.7	201.5
10			12.25	225.8
11			12.15	219.7
12			12.15	197
13		0.3×0.36×0.12	7.78	141.7
14			7.6	122.7
15			7.26	150
16			7.08	125.8
17			7.08	116.7
18			6.95	137.9

6.2 Comparison between double-K fracture parameters and double-G counterpart

From the analysis of double-*G* fracture model, it can be said that though based on the energy method, it is essentially equivalent to stress intensity-oriented double-*K* fracture model since both of them adopt LEFM in conjunction with fictitious crack model. Then fracture parameters introduced in these two methods should follow certain relations as in LEFM. Next the numerical comparisons of these parameters are made to justify this argument.

Here comparative parameter $\widetilde{K}$ corresponding to energy release rate G is inducted denoting the stress intensity factor corresponding to G from LEFM

$$\widetilde{K}=\sqrt{G\times E} \tag{16}$$

where E is the elastic modulus of material. Through the above equation, the double-*G* fracture toughness will be transformed into the pattern of stress intensity factor: $\widetilde{K}_{\mathrm{Ic}}^{\mathrm{ini}}$ $\widetilde{K}_{\mathrm{Ic}}^{\mathrm{un}}$, which will be compared with double-*K* fracture toughness $K_{\mathrm{Ic}}^{\mathrm{ini}}$ and $K_{\mathrm{Ic}}^{\mathrm{un}}$ (Zhao, 2002). The computation results are tabulated in Table 2. To see it intuitionisticly, comparative graph is also given in Fig.6.

Table 2 The calculated results of double *G* from CT specimen

	$G_{\mathrm{Ic}}^{\mathrm{un}}$ (N/m)	$G_{\mathrm{Ic}}^{\mathrm{ini}}$ (N/m)	$\widetilde{K}_{\mathrm{Ic}}^{\mathrm{ini}}$ (MPam$^{1/2}$)	$\widetilde{K}_{\mathrm{Ic}}^{\mathrm{un}}$ (MPam$^{1/2}$)
1	156.92	94.54	1.686	2.206
2	127.05	70.28	1.437	1.985
3	165.31	100.74	1.735	2.264
4	159.60	93.23	1.686	2.224
5	124.24	67.99	1.395	1.963
6	108.62	53.60	1.226	1.835
Ave.	140.29	80.06	1.527	2.079
7	114.16	64.25	1.350	1.881
8	120.77	66.05	1.407	1.935
9	101.60	53.42	1.224	1.775
10	116.26	62.77	1.352	1.898
11	110.67	56.23	1.296	1.852
12	95.90	48.34	1.151	1.724
Ave.	109.89	58.51	1.297	1.844
13	92.25	48.82	1.169	1.691
14	74.47	34.65	0.970	1.519
15	95.11	48.70	1.180	1.717
16	73.35	30.39	0.926	1.508
17	66.67	25.37	0.849	1.438
18	82.77	38.77	1.033	1.602
Ave.	80.77	37.78	1.021	1.579

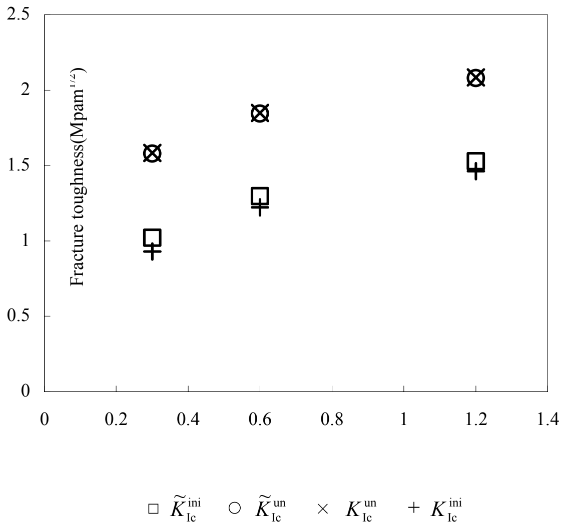

Fig.6 The comparison between the double *K* and double *G* parameters

From Fig.6 and Table2, it is observed that for concrete materials, the double-*K* fracture toughness $K_{\mathrm{Ic}}^{\mathrm{ini}}$ and $K_{\mathrm{Ic}}^{\mathrm{un}}$ and their counterpart $G_{\mathrm{Ic}}^{\mathrm{ini}}$ and $G_{\mathrm{Ic}}^{\mathrm{un}}$ in double-*G* fracture model still obey the LEFM law shown in Eq.(16), which confirms the equivalence of stress intensity method and energy method in describing the fracture behavior of concrete materials.

7 CONCLUSION

From the energy consideration, double-*G* fracture criterion is established with energy-based fracture toughness G_{Ic}^{ini} and G_{Ic}^{un} as the fracture parameters, where G_{Ic}^{ini} represents the inherent energy necessary for crack initiation in the absence of FPZ, while G_{Ic}^{un} denotes the resistance of material to the unstable propagation. Both of these two parameters can be theoretically given through the LEFM. Given the difficulty in capturing the initial crack load P_{ini}, an alternative for estimating G_{Ic}^{ini} is given by considering the energy consumption G_{Ic}^{c} contributed by cohesive force distributed over the FPZ. The very existence of FPZ ahead of the free-crack tip is responsible for the nonlinearity observed in the load-displacement response, and the fracture process is inevitably accompanied by energy consumption G_{Ic}^{c} over FPZ, which is intimately related to the constitutive relations along the FPZ.

Double-*G* fracture criterion is the counterpart of double-*K* fracture model which accepts the stress intensity factor as the quantity to describe the fracture behavior of concrete materials. Both of them are established on the presumption of linear asymptotic superposition, meaning they essentially based on linear elastic fracture mechanics, which ensure the equivalence of these two approaches in fracture mechanics of concrete. This point is verified by the comparison of the corresponding fracture parameters obtained through the compact tension specimens.

Acknowledgements: This paper is supported by the National Key Basic Research and Development Program (973 Program) No. 2002CB412709. The authors also wish to thank the NSFC (Natural Science Foundation of China) for their supports (Grants No.10272068 and No.50178015)

References

ASTM Standard E399-72. 1972. Standard method of test for plane-strain fracture toughness of metallic materials. Annual Book of ASTM Standards.

Bažant Z.P. 1983. Crack band theory for fracture of concrete. *RILEM. Materials and Structures* 16(93): 155-177.

Bažant Z.P. 1986. Determination of fracture properties from size effect tests. *Journal of Structural Engineering, ASCE* 112(2): 289-307.

Bažant Z.P. 1996. Analysis of work-of-fracture method for measuring fracture energy of concrete. *Journal of Engineering Mechanics* 122(2): 138-144.

CEB-Comite Euro-International du Beton- EB-FIP Model Code 1990, Bulletin D'Information No.213/214, Lausanne, 1993.

Hillerborg A. 1976. Analysis of crack formation and crack growth in concrete by means of fracture mechanics and finite elements. *Cement and Concrete Research* 6: 773-782.

Jenq Y.S & Shah S.P. 1985. Two parameter fracture model for concrete. *Journal of Engineering Mechanics*, ASCE, 111(10): 1227-1241.

Karihaloo B.L & Nallathambi P. 1990. Effective crack model for the determination of fracture toughness K_{Ic}^{s} of concrete. *Engineering Fracture Mechanics* 35(4/5): 637-645.

Murakami(Editor-in-chief). Stress Intensity Factors Handbook. Pergamon Press, London, 1987

Nallathambi P. & Karihaloo B.L. et. 1984. Al. Effect of specimen and crack sizes, water/cement ratio and coarse aggregate texture upon fracture toughness of concrete. *Magazine of Concrete Research* 36(129): 227-236.

Refai T.M.E & Swartz S.E. 1987. Fracture behavior of concrete beams in three-point bending considering the influence of size effects. *Report No.190, Engineering Experiments Station*, Kansas State University.

Shilang Xu. 1999. Determinaiton of parameters in the bilinear, Reinhardt's and exponentially nonlinear softening curves and their physical meanings. Werkstoffe und Werkstoffprüfung im bauwesen, Hamburg, Libri BOD: 410-424.

Xu S. & Reinhardt H.W. 1999. Determination of double-K criterion for crack propagation in quasi-brittle fracture, Part I: Experimental investigation of crack propagation, *International Journal of Fracture* 98: 111-149,

Xu Shilang & Reinhardt H.W. 1998. Crack extension resistance and fracture properties of quasi-brittle softening materials like concrete based on the complete process of fracture. *International Journal of Fracture* 92: 71-99.

Xu Shilang & Reinhardt H.W. 1999. Determination of double-K criterion for crack propagation in quasi-brittle fracture, Part Ⅲ: compact tension specimens and wedge splitting specimens. *International Journal of Fracture* 98: 179-193.

Xu Shilang, 2002. The calculation approach of double-K fracture parameters of concrete and a possible coding standard test method for determining them, *Journal of China Three Gorges University* 24(1): 1-8.

Zhao Yanhua, 2002. The analytical study on the energy in the fracture process of concrete, Doctoral dissertation, Dalian University of Technology.